



Identification of new Omega-3 very long chain poly-unsaturated fatty acids in meibomian gland secretions

Romain Magny^{a, b, *}, Anne Regazzetti^b, Karima Kessal^{a, c}, Orane Christin^b, Christophe Baudouin^{a, c, d}, Emmanuel Roulland^b, Françoise Brignole-Baudouin^{a, b, e}, Olivier Laprévote^{b, f}, Nicolas Auzeil^{b, **}

^a Sorbonne Université UMR80, INSERM UMR 968, CNRS UMR 7210, Institut de la Vision, IHU ForeSight, 75012, Paris, France

^b Université Paris Cité, CNRS, CITCoM, F-75006, Paris, France

^c CIC 1423, Centre Hospitalier National d'Ophtalmologie des Quinze-Vingts, IHU ForeSight, 75012, Paris, France

^d Hôpital Ambroise Paré, AP-HP, Université Versailles St Quentin en Yvelines, Paris Saclay, 78180, Montigny-Le-Bretonneux, France

^e Laboratoire d'ophtalmobiologie, Centre Hospitalier National d'Ophtalmologie des Quinze-Vingts, IHU ForeSight, 75012, Paris, France

^f Hôpital Européen Georges Pompidou, AP-HP, Service de Biochimie, 75015, Paris, France

ARTICLE INFO

Article history:

Received 3 January 2022

Received in revised form

14 March 2022

Accepted 19 April 2022

Available online 25 April 2022

Keywords:

Lipid identification

Molecular network

Tandem mass spectrometry

Ocular surface

Meibum

Cross metathesis

ABSTRACT

Three new very long chain polyunsaturated fatty acids (VLC PUFA) belonging to the omega-3 family have been identified in meibum samples collected by Schirmer strips. These VLC PUFA, namely FA (32:3), FA (34:3) and FA (36:3), were detected in O-acyl- ω -hydroxy fatty acids using a molecular network approach, and as free fatty acids. Identification was supported by retention time prediction model, exact mass determination and isotopic patterns. Double bond location was determined using cross metathesis reaction associated to tandem mass spectrometry. In meibum, synthesis of these VLC PUFA is likely to be mediated by elongation of very long chain fatty acids 4 enzyme. The biological role of these newly VLC PUFA and their occurrence in other tissues and biological fluids remains to be elucidated.

© 2022 Elsevier B.V. and Société Française de Biochimie et Biologie Moléculaire (SFBMM). All rights reserved.

1. Introduction

Meibum is a lipid secretion produced by meibomian glands, which are located in the tarsal plate of eyelids in humans and other mammals [1]. This lipids mixture makes part of the tear film namely the outer tear film lipid layer covering the two other layers, the aqueous and mucin layers [2]. Tear film spreads over the entire anterior surface of the eye, and its stability may be regarded as a hallmark of ocular surface homeostasis. A quality defect of tear film has been reported for decades in the pathogenesis of ocular surface diseases such as dry eye disease (DED) [2]. Indeed, meibomian gland dysfunction alters the meibum composition leading to tear

film instability, a key feature of DED [3]. Numerous studies have described the changes in the lipid composition of meibum in patients with DED in order to better understand the pathology and to identify new biomarker candidates improving the diagnosis of the disease [4–6]. Qualitative studies were also performed to characterize the broad array of molecular diversity of meibum lipids [1,7]. Lipids secreted by meibomian glands include wax esters, cholesterol esters, O-acyl- ω -hydroxy fatty acids (OAHFA) and diacylated fatty α,ω -diols (DiAD) (Fig. 1) [7]. Their high hydrophobic property makes them essential to prevent tear film evaporation thus contributing to maintain the ocular surface health [8]. Beside fatty acids commonly encountered within lipid subclasses, meibum lipids also contain very long chain fatty acids (VLC FA). VLC FA are defined as FA containing between 22 and 36 carbons. In meibum, VLC FA are known to contribute to increase hydrophobicity [9,10]. The VLC FA previously described in meibum are mostly saturated or mono-unsaturated e.g. FA (30:0), FA (30:1), FA (32:1) [11]. VLC FA are encounter as esterified in cholesterol esters, OAHFA and DiAD

* Corresponding author. Sorbonne Université UMR80, INSERM UMR 968, CNRS UMR 7210, Institut de la Vision, IHU ForeSight, 75012, Paris, France. .

** Corresponding author.

E-mail addresses: romain.magny@inserm.fr (R. Magny), nicolas.auzeil@u-paris.fr (N. Auzeil).

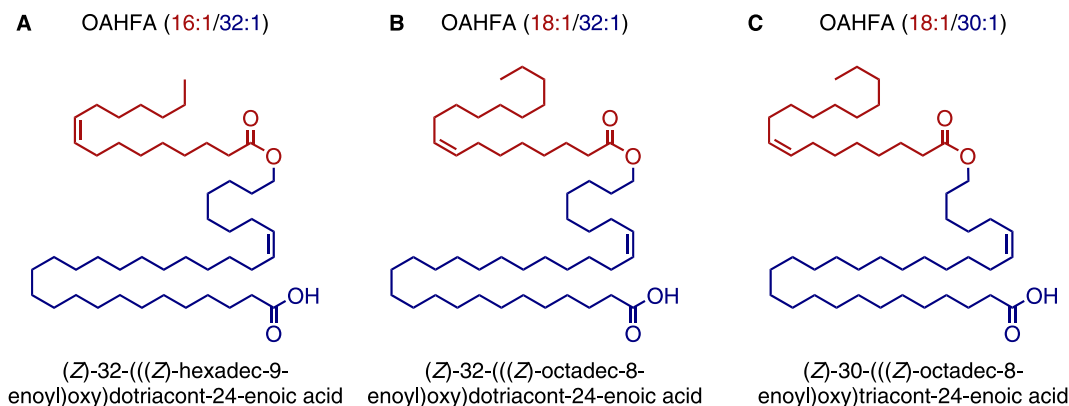


Fig. 1. Chemical structure of three O-Acyl Hydroxylated Fatty Acids (OAHA) encountered in meibum. (A) OAHA (16:1/32:1), (B) OAHA (18:1/32:1) and (C) OAHA (18:1/30:1).

especially in meibum. In previous studies, we investigated lipid changes in an *in vitro* cell model of DED using a comprehensive untargeted lipidomic analysis [12]. In addition, the reliable identification of the numerous lipid species down to the fatty acid side chain composition and sn_1/sn_2 location was achieved thanks to molecular networking [12]. Using this approach, more than 300 lipid species were identified in the human corneal cell line studied [13].

In the present study, we would like to report identification of three new very long chain fatty acids discovered during an analysis of lipids secreted by the meibomian glands using an untargeted lipidomic analysis combined with molecular networks. Meibomian lipid secretions were collected using Schirmer Strips according to previously published studies [8].

2. Material and methods

2.1. Chemicals and reagents

Chloroform (Carlo Erba Reactifs SDS, Val-de-Reuil, France), acetonitrile, methanol, isopropanol, water of LC-MS grade (J.T. Baker, Phillipsburg, NJ, USA) and 3,5-di-*tert*-4-butylhydroxytoluene (Sigma Aldrich, Saint-Quentin Fallavier, France) were used to perform lipid extraction and to prepare mobile phase for liquid chromatography. All commercial lipid standards were purchased from Avanti Polar Lipids, Inc. (Alabaster, AL, USA). Cross-metathesis reactions were performed under an argon atmosphere in anhydrous dichloromethane (CH_2Cl_2). Anhydrous CH_2Cl_2 was obtained through distillation over CaH_2 under argon.

2.2. Lipid extraction

Ocular surface samples were collected using Schirmer strips (ScS) (Dina strip Schirmer-Plus®, Gecis, Lamotte-Beuvron, France) without anesthesia from both eyes of healthy volunteers ($n = 8$) taking care that the strips do not touch the skin and were immediately stored at -80°C until handle. The study was performed according to the tenets of the Declaration of Helsinki and GCP, and written consent was obtained from all subjects after explaining the protocol and the scope of the study. The study was approved by the Ethics Committee CPP-Ile-de-France (number: 2018-A02800-55).

Desorption of lipids was performed in borosilicated tubes by immersing ScS in 900 μL of ice-cold $\text{CHCl}_3/\text{MeOH}$ (1/2, v/v) and stirred overnight at 4°C using a thermomixer set at 1200 rpm, as previously described [8]. Water (540 μL) and CHCl_3 (300 μL) were subsequently added, and phase separation was achieved through centrifugation at 3000 rpm for 10 min. Organic phases were then

collected, and solvents were evaporated under reduced pressure at 45°C .

2.3. Double bond location

Double bond location was performed using combination of cross metathesis (CM) reaction and mass spectrometry analysis following the method we previously described [14]. Briefly, a Schlenk tube charged with Grubbs' catalyst of second generation (12.2 mg, 0.014 mmol), was flushed with argon and CH_2Cl_2 (2 mL) and (Z)-but-2-ene-1,4-diyl diacetate (114 μL , 0.715 mmol) were added. The solution was stirred at 40°C for 2 h and diluted to 1/1000 using dry CH_2Cl_2 under argon. The diluted solution (300 μL) was subsequently added to the extracted lipids pre-treated with 1 M HCl and the solvent was evaporated to dryness under argon and heated at 40°C for 4 h. The residue was reconstituted in 100 μL of a $\text{CHCl}_3/\text{ACN}/\text{H}_2\text{O}/\text{IPA}$ (20/30/10/30, v/v/v/v) mixture and 5 μL were injected in the LC-MS/MS system.

2.4. Data-dependent LC-ESI-HRMS/MS analysis

The analysis of lipid extracts was performed by liquid chromatography hyphenated to mass spectrometry. Ionization was achieved by positive and negative electrospray using a Synapt® G2 (Q-TOF) mass spectrometer (Waters, Manchester, UK). The chromatographic separation was performed at 50°C on an Acquity® CSH C18 column (100 mm \times 2.1 mm; 1.7 μm) using a binary solvent gradient system which consists in 10 mM ammonium acetate in acetonitrile/water mixture (40:60, v/v) as solvent A and 10 mM ammonium acetate in acetonitrile/isopropanol mixture (10:90, v/v) as solvent B. Solvent B increased from 40% to 100% in 10 min, was held at 100% for 2 min before returning to 40%. The flow rate was kept at 0.4 mL min^{-1} . The ionization source parameters were as follows: capillary voltage 3000 V (ESI+) and 2400 V (ESI−), cone voltage 30 V (ESI+) and 45 V (ESI−), source temperature 120°C , desolvation temperature 550°C , cone gas flow 20 L h^{-1} , and desolvation gas flow 1000 L h^{-1} . Leucine enkephalin (2 ng mL^{-1}) was used as an external reference compound (Lock-Spray™) for mass correction. Data-dependent acquisition (DDA) was performed as follows: a full MS scan was first acquired and was followed by 5 MS/MS scans obtained from the most intense ions above an absolute threshold of 500 counts. These precursor ions were selected by the quadrupole set at a window size of 1.5 Thomson and fragmented using a collision energy ramping from 20 to 40 eV. The scan duration of MS and MS/MS spectra was set at 0.2 s. Data were acquired in the full scan mode between m/z 50 and 1200 using a resolution of 20,000 FWHM at m/z 500. Data acquisition was

managed using Waters MassLynx™ software (version 4.1; Waters MS Technologies).

2.5. Data-preprocessing parameters

Raw data files acquired in positive and negative ion modes were converted into open source mzXML files under MSConvert 3.0. The data-processing was performed under MZmine 2.53 as previously described [12,13]. Briefly, MS and MS/MS spectra were extracted using a mass detection noise level set at 1E2 and 0E0, respectively. Chromatograms were built using the ADAP algorithms (minimum group size of 5 scans, a group intensity threshold of 1,000, and an m/z tolerance of 10 ppm) [15]. ADAP wavelets chromatogram deconvolution algorithm was set at the following parameters: signal to noise ratio = 10, coefficient/area ratio = 120, peak duration range = 0.05–0.5 min, retention time wavelet range = 0.0–0.2. De-isotope chromatograms were generated using the isotopic peaks grouper algorithm set at m/z and t_R tolerance of 10 ppm and 0.1 min, respectively. Peak alignment was achieved using join aligner method with parameters set at m/z and t_R tolerance of 10 ppm and 0.15 min, respectively. MS/MS scans were associated to the corresponding MS scans using a m/z and t_R tolerance of 10 ppm and 0.15 min, respectively. Gap-filling process was performed on the peak list using the so-called module “same RT and m/z range gap filler” with m/z tolerance of 10 ppm. Lipids were annotated based on exact mass measurement and retention time with the “custom database” module using an in-house database. Data pre-processing procedures led to one matrix in ESI+ and one in ESI-, listing m/z , t_R and peak area values for annotated lipids. Matrixes were finally normalized and filtered as previously described [16,17].

2.6. Molecular network (MN) creation

The MNs were generated using the feature based molecular networking workflow of the Global Natural Products Social (GNPS) platform and using MetGem software [18,19]. The following settings were used to build the network: minimum pairs Cos >0.60, parent ion mass tolerance = 0.02 Da, fragment ion mass tolerance = 0.02, network topK <150, minimum matched peaks = 4, and minimum cluster size = 2. The library spectra inquiries were performed using the same parameter values as those define for the network building. The MNs were finally visualized and annotated using Cytoscape 3.4.0 software (San Diego, California, USA) [20].

2.7. Identification of lipids

The structure assignment of lipid species was based on MS and MS/MS data, using a tolerance window of 5 and 15 ppm, respectively. Identification was supported by comparison of experimental t_R values to empirical values calculated using t_R prediction models. MS/MS data was used to fully determine fatty acid composition. The identification of lipids at the fatty acid side chain level was followed by cross metathesis products analysis to identify the double bond location within fatty acid side chains. The structure assignment of cross-metathesis products was also based on MS and MS/MS data using a tolerance window of 5 and 15 ppm, respectively. For all the lipid species, the side chain was identified thanks to MS/MS data in negative ion mode.

3. Results and discussion

In the present study, we described for the first time three novel omega-3 very long chain fatty acids (VLC FA) identified during an untargeted lipidomic analysis performed on Schirmer Strips (ScS)

samples. The analytical procedure included a Bligh and Dyer liquid-liquid extraction followed by sample analysis using reversed-phase liquid chromatography hyphenated to high resolution tandem mass spectrometry (LC-ESI-HRMS/MS). It makes it possible to cover detection and quantification of lipids exhibiting a large structural diversity and a wide concentration range [17]. To ensure a reliable identification of lipid species detected and quantified, a procedure based on MS, MS/MS and t_R data analyses was developed. Moreover, polar head group identification and fatty acyl side chain location within lipid species, were achieved based on molecular networks (MN) and GNPS database querying, as previously described [12]. Eventually, double bond location was performed thanks to MS/MS data analyses of cross metathesis products, we recently published [14].

Lipidomic data obtained thanks to LC-ESI-HRMS/MS from ScS lipid extracts were used to generate molecular networks (Fig. 2A). In a previous study, we exhaustively described the contribution of MN in the identification of lipids [12]. MN approach was also used in the present study. In negative ion mode, networking was based on sphingosine moiety thus clustering ceramide species (Fig. 2A). Network was also based on acetate adducts ($[M + CH_3COO]^-$) clustering phosphatidylcholines (PC) and sphingomyelins (SM). Indeed, PC and SM acetate adducts undergone neutral loss of methyl acetate displayed on MS/MS spectra. Besides being based on lipid subclasses, a network was built on the nature of fatty acyl side chains. Indeed, diacyl phosphatidylethanolamine (PE) and alkylacyl phosphatidylethanolamine (PE-O) are clustered in the same MN since they share a common fatty acyl side chain (Fig. 2B). This network also clustered O-Acyl- ω -Hydroxy Fatty Acids (OAHFA) lipid species, some of them being linked to phospholipids since their MS/MS spectra shared common product ions especially carboxylate ions. For instance, PE (18:1/18:1) was connected to OAHFA (18:1/24:1) and PE (18:0/18:1) to OAHFA (18:1/34:1) as they both contain an octadecenoate fatty acyl side chain (Fig. 2B). The propagation of the annotation, namely identification of both hydroxylated fatty acids and fatty acids, clustered in MN was performed for 34 OAHFA (Supplementary Table 1). It included two O-acyl- ω -hydroxy fatty acids, OAHFA (50:4) and OAHFA (52:4), containing new FA previously undescribed. MS/MS spectra of the former displayed a peak at m/z 281.2341, corresponding to an octadecenoate (FA 18:1) (Fig. 2C). It was supported by the fact that OAHFA (50:4) was linked to OAHFA (18:1/24:1), OAHFA (18:1/32:2) and OAHFA (18:1/30:2) (Fig. 2D, E, 2F). Moreover, MS/MS spectra of OAHFA (50:4) showed a second peak at m/z 489.4313 which could be assigned to an ω -hydroxy FA (32:3) allowing to annotate OAHFA (50:4) as OAHFA (18:1/32:3) (Fig. 2C). OAHFA (18:1/32:3) biosynthesis involves condensation of FA (18:1) and ω -hydroxy FA (32:3), which in turn originates from the oxidation of FA (32:3) mediated by a cytochrome P450 [21]. The ω -hydroxy FA are known to be low abundant species and were not detected in our samples whatever the OAHFA considered [22]. In contrast, free FA, the corresponding biosynthetic precursors, can be easily detected e.g. FA (30:1), FA (32:1) and FA (34:1) for OAHFA (18:1/30:1), OAHFA (18:1/32:1) and OAHFA (18:1/34:1), respectively. To our knowledge, FA (32:3), the biosynthetic precursor of OAHFA (18:1/32:3), was not previously described in any database e.g. LipidMaps or Human Metabolome Database (HMDB). The question arose if ScS lipid extract also contained FA (32:3) as free fatty acids. Additional data analyses were thus performed. Unfortunately, MS/MS spectra data are poorly informative regarding free fatty acids and no MN based on free FA can indeed be generated [23]. Nevertheless, the extracted ion chromatogram (EIC) at m/z 473.4360, corresponding to $[M - H]^-$ of FA (32:3), displayed a peak at t_R = 7.01 min suggesting that ScS samples contained this FA as free species (Fig. 3A). In addition, the difference between experimental and theoretical m/z values was

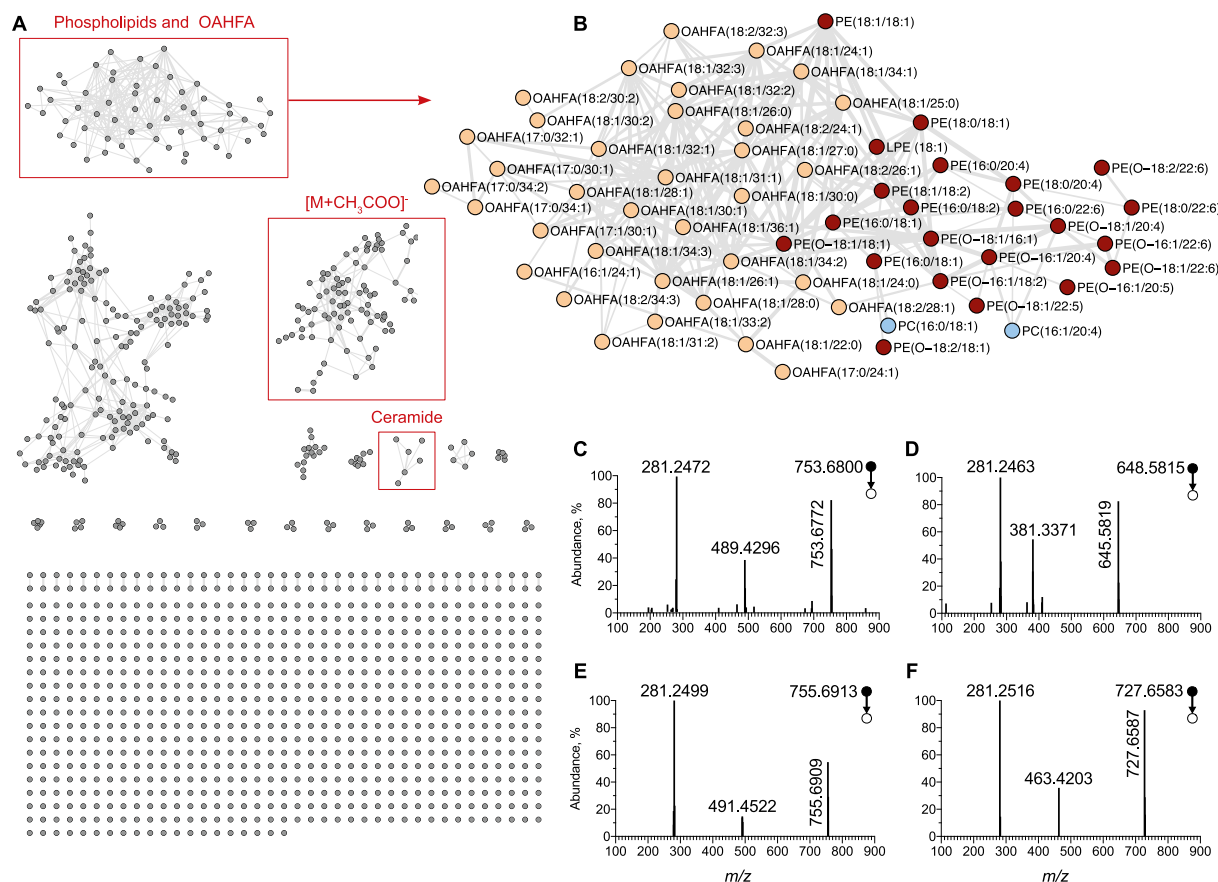


Fig. 2. Molecular network generated from LC-ESI-HRMS/MS data of lipid extracts from Schirmer strips. The MN were generated using MetGem software. (A) Global molecular network displaying clusters corresponding to $[M + CH_3COO]^+$ adducts, phospholipids and O-acyl- ω -hydroxy fatty acids (OAHFA) subclasses and ceramides. (B) Sub-network cluster of PE and OAHFA sharing common fatty acyl side chains. MS/MS spectra of (C) OAHFA (18:1/32:3), (D) OAHFA (18:1/24:1), (E) OAHFA (18:1/32:2) and (F) OAHFA (18:1/30:2).

1.5 ppm and the isotopic pattern indicated a molecular formula of $C_{32}H_{58}O_2$ consistent with FA (32:3). Chromatographic data are valuable to support identification of lipid species since it is well known that the equivalent carbon number (ECN) is tightly correlated to retention time (t_R) and thus widely used in the context of a lipidomic analyses [16,24,25]. Annotation of FA (32:3) was therefore supported by investigating chromatographic data. For this purpose, experimental t_R of known FA contained in ScS were plotted to the corresponding ECN values to generate the t_R prediction model, as previously described (Fig. 3B) [16,24,25]. It is noteworthy that under our chromatographic conditions, the best correlation between experimental t_R and ECN was achieved using a polynomial fitting (third order) (Fig. 3B). The experimental t_R of FA (32:3) measured on EIC at m/z 473.4360 were compared to the empirical t_R value obtained thanks to the t_R prediction model. A difference of 1% was displayed, supporting the proposed annotation (Fig. 3B).

In a similar way, OAHFA (52:4) was annotated as OAHFA (18:1/34:3). Indeed, the MS/MS spectra displayed a peak at m/z 281.2461, indicative of an octadecenate side chain, while a second one at m/z 517.4557 would correspond to an ω -hydroxy FA (34:3). ScS samples also contained FA (34:3), the biosynthetic precursor of OAHFA (18:1/34:3), as free fatty acid. Indeed, a peak at m/z 501.4670 and $t_R = 7.42$ min corresponding to the $[M - H]^-$ of FA (34:3) was detected, respectively at 2 ppm from its theoretical m/z value and 1% of its empirical t_R (Fig. 3C and E). In addition, the isotopic pattern was consistent with the molecular formula of FA (34:3). A

systematic inspection of LC-ESI-HRMS/MS data for the occurrence of other FA not previously described indicated that ScS lipid extracts also contained FA (36:3) (Fig. 3D). This FA was annotated following the analytical procedure used for FA (32:3) and FA (34:3). It is worth to notify that no OAHFA containing ω -hydroxy FA (36:3) was detected.

The three FA newly annotated belong to the VLC FA family since they contain more than 22 carbons. To complete the annotation, an attempt to identify the double bond location was performed using the procedure based on cross metathesis (CM) reaction and tandem mass spectrometry analysis we previously described [14]. Cross-metathesis is a common organic reaction implementing metal-carbene catalysis that allows exchanging fragments between molecules via the selective reaction of their alkene function. Briefly, the ScS lipid extract was treated with Grubb's catalyst and butene diacetate during 4 h at 40 °C and subsequently analyzed by LC-MS/MS. Regarding FA (34:3), chromatographic and MS data analysis led to the detection of three CM products: FA (OAc-33:3 $\Delta 27$ $\Delta 30$ $\Delta 33$) at m/z 545.4575 and $t_R = 6.28$ min, FA (OAc-32:2 $\Delta 27$ $\Delta 30$) at m/z 505.4262 and $t_R = 5.78$ min and FA (OAc-29:1 $\Delta 27$) at m/z 465.4002 and $t_R = 5.34$ min (Fig. 4). These three CM products allowed to propose a double bonds location at $\Delta 25$ $\Delta 28$ $\Delta 31$ positions. FA (34:3) thus belong to the ω -3 fatty acids family. In a same manner, the three CM products of FA (36:3), namely FA (37:3-OAc $\Delta 27$ $\Delta 30$ $\Delta 33$), FA (34:2-OAc $\Delta 27$ $\Delta 30$) and FA (31:1-OAc $\Delta 27$) were detected at m/z 573.4888 and $t_R = 6.73$, at m/z 533.4575 and $t_R = 6.33$ and at m/z 493.4262 and $t_R = 6.05$, respectively (Fig. 4). Finally, FA (33:3-

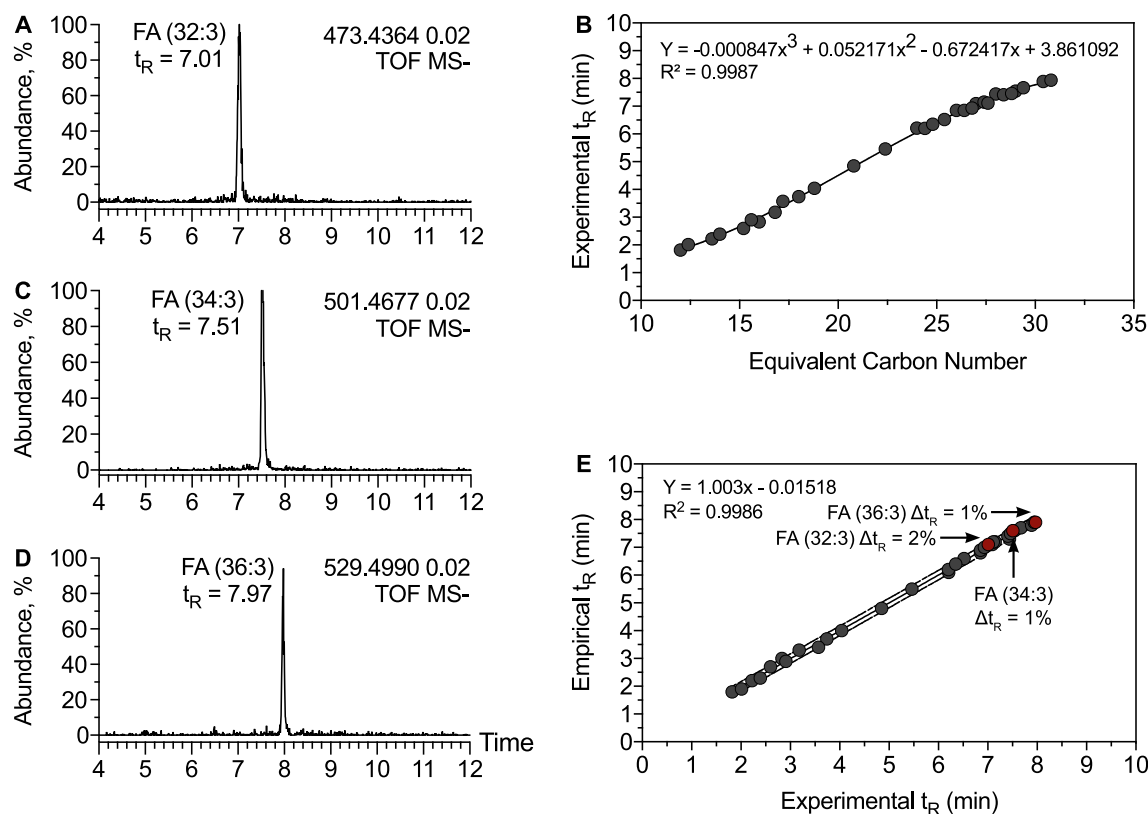


Fig. 3. Chromatographic data of FA (32:3), FA (34:3) and FA (36:3). (A) Extracted ion chromatogram (EIC) of ScS lipid extract at m/z 473.4364 corresponding to the $[M - H]^-$ ion of FA (32:3). (B) Retention time prediction model based on equivalent carbon number (ECN) for FA subclass. A polynomial (third order) regression model was used. (C and D) EIC of ScS lipid extract at m/z 501.4677 and m/z 529.4990 corresponding to the $[M - H]^-$ ion of FA (34:3) and FA (36:3), respectively. (E) Empirical t_R plotted against experimental t_R for all FA identified in ScS samples including FA (32:3), FA (34:3) and FA (36:3). Note that the difference between experimental and empirical t_R values do not exceed 2% for FA (32:3), FA (34:3) and FA (36:3).

	n	C1		C2		C3	
		t_R	m/z (Δ ppm)	t_R	m/z (Δ ppm)	t_R	m/z (Δ ppm)
FA (32:3)	0	5.37	517.4262 (3)	5.11	477.3949 (3)	4.70	437.3636 (2)
FA (34:3)	2	6.28	545.4575 (3)	5.78	505.4262 (2)	5.34	465.4002 (0)
FA (36:3)	4	6.73	573.4888 (3)	6.33	533.4575 (2)	6.05	493.4262 (2)

Fig. 4. Chromatographic and MS data of cross metathesis products of FA (32:3), FA (34:3) and FA (36:3). Structure of VLC PUFA belonging to the ω -3 family. Table including chromatographic and MS data of cross metathesis products of FA (32:3), FA (34:3) and FA (36:3). The table also indicates the difference between experimental and theoretical m/z values in ppm for each cross-metathesis product.

OAc Δ 25 Δ 28 Δ 31), FA (30:2-OAc Δ 25 Δ 28) and FA (27:1-OAc Δ 25), respectively at m/z 517.4262 and $t_R = 5.37$, at m/z 477.3949 and $t_R = 5.11$ and at m/z 437.3636 and $t_R = 4.70$ was identified as CM products of FA (32:3) (Fig. 4). Consequently, FA (32:3), FA (34:3) and FA (36:3) belong to the ω -3 fatty acids family. It must be emphasized that, when double bond location in lipids included in a complex biological sample is based on CM, the distal part of the native lipid is lost. The presence of other minor isomers having

different double bond location, especially those belonging to ω -6 fatty acid family, thus cannot be excluded.

Regarding the double bond stereochemistry of the FA (32:3), FA (34:3) and FA (36:3), direct evidence remains difficult to obtain without chemical standards. Nevertheless, it must be emphasized that, in mammalian organisms, double bonds display a *cis* stereochemistry in mono-unsaturated FA and poly-unsaturated FA. Furthermore, some experimental indirect evidence may indicate

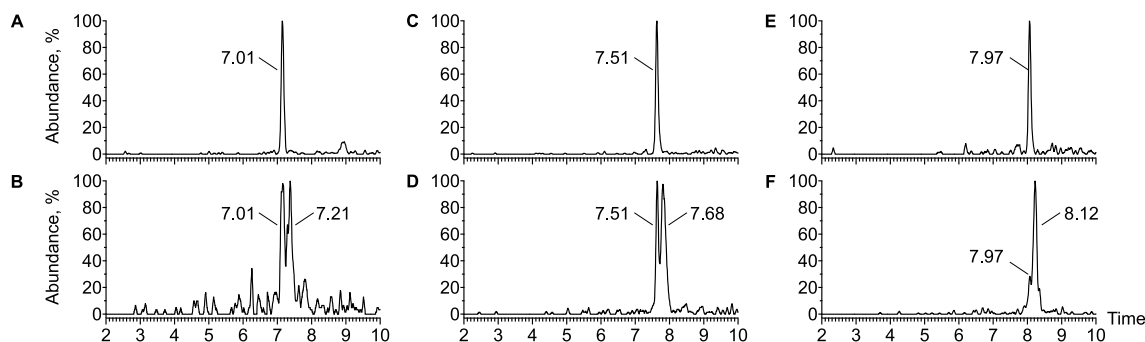


Fig. 5. Isomerization of FA (32:3), FA (34:3) and FA (36:3) during CM reaction. Extracted ion chromatogram (EIC) of ScS lipid extract at m/z 473.4364 corresponding to the $[M - H]^-$ ion of FA (32:3) (A) before and (B) after CM reaction. EIC of ScS lipid extract at m/z 501.4677 corresponding to the $[M - H]^-$ ion of FA (34:3) (C) before and (D) after CM reaction. EIC of ScS lipid extract at m/z 529.4990 corresponding to the $[M - H]^-$ ion of FA (36:3) (E) before and (F) after CM reaction.

that FA (32:3), FA (34:3) and FA (36:3) are *all-cis*. Under our chromatographic conditions, a unique peak corresponding to the $[M - H]^-$ ion was displayed on the EIC whatever the FA considered (Fig. 3A, C and 3D), suggesting that they all exhibit a unique stereochemistry. *Z* and *E*-stereoisomeric fatty acids (or fatty-acyl containing lipids) are indeed usually separated under our chromatographic conditions. For instance, EIC at m/z 281.2480 corresponding to the $[M - H]^-$ ion of *Z*- and *E*-oleic acid displayed two well-separated peaks at $t_R = 3.11$ min and $t_R = 3.33$ min, respectively (data not shown). The chromatographic separation of *Z* and *E*-stereoisomeric fatty acids were also displayed for polyunsaturated fatty acid *i.e.* arachidonic acid. Indeed, for FA (20:4), following cross metathesis reaction, peaks corresponding to stereoisomers are displayed on the chromatogram at $t_R = 2.54$ min and $t_R = 2.83$ min (Supplementary Fig. S2). Among these peaks, one is markedly more intense and may consequently be attributed to the more thermodynamically stable *all-trans* species since cross metathesis reaction is predominantly performed under thermodynamic control. In addition, in the same chromatographic conditions, PG (18:1/18:1) *all-cis* and *all-trans* were eluted at $t_R = 6.70$ min and $t_R = 7.00$ min respectively [26]. A further indirect evidence is provided by the fact that, during cross-metathesis, *cis* to *trans* double bond isomerization was reported [27,28]. For instance, while native FA (36:3) exhibited a unique peak at $t_R = 8.06$ min, two peaks at $t_R = 8.06$ min

and $t_R = 8.21$ min were displayed on EIC of the CM products at m/z 501.4677 (Fig. 5). Altogether, these results strongly suggest that the stereochemistry of the native FA (36:3) is *all-cis*. Using the same approach, FA (32:3) and FA (36:3) were assigned the structure *all-cis* (Fig. 5).

The fact that VLC PUFA, FA (32:3), FA (34:3) and FA (36:3), were detected in ScS samples supports their meibomian origin [5]. Indeed, these lipid species were also present in pure meibum samples (data not shown). To our knowledge, in contrast to VLC SFA and VLC MUFA, this is the first time that VLC PUFA have been detected in meibum [7,11]. VLC FA synthesis is mediated by elongation of very long chain fatty acids (ELOVL) enzyme, especially ELOVL4, which is localized within the meibomian gland [7,9,11]. Similarly to VLC SFA and VLC MUFA, which were identified in our study, FA (32:3) and FA (34:3) were mainly detected as OAHFA, cholesteryl esters and, to a less extent, as free fatty acids (Fig. 6 and Supplementary Fig. S2). In contrast, FA (36:3) was only detected as free fatty acids and was the less abundant one compared to FA (32:3) and FA (34:3). This could explain why in ScS lipid extract, it was not detected neither as OAHFA nor as cholesteryl ester. The biological role of FA (32:3), FA (34:3) and FA (36:3) remains to be elucidated. Nevertheless, in a mouse model harboring mutation in *ELOVL4* gene, a decrease of VLC SFA has been associated with an increase in eyelid blink rates and a decrease in keeping their eyelids

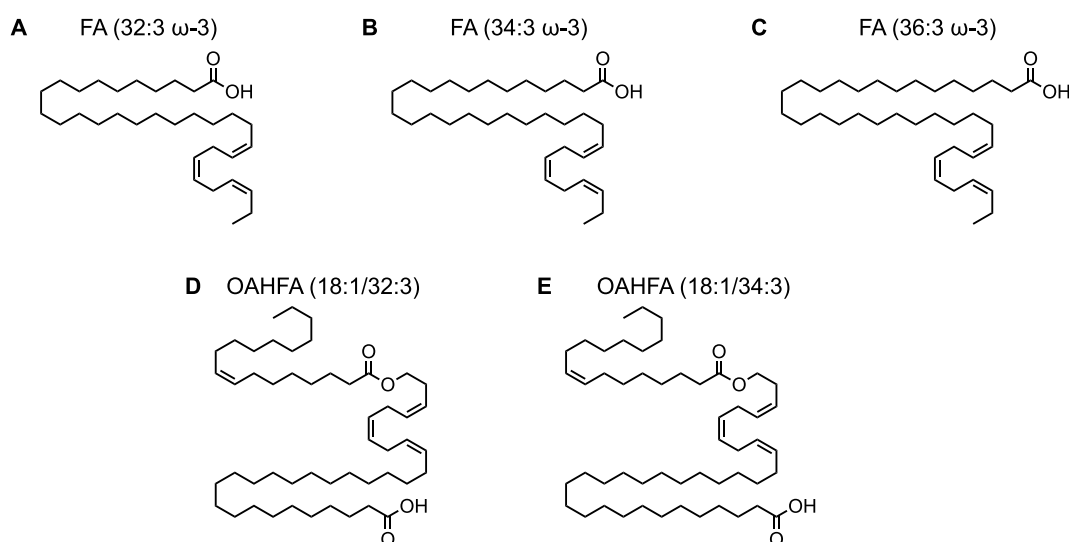


Fig. 6. Structure of identified FA and their corresponding O-acyl- ω -hydroxy fatty acids (OAHFA). Structure of (A) FA (32:3), (B) FA (34:3), (C) FA (36:3), (D) OAHFA (18:1/32:3) and (E) OAHFA (18:1/34:3).

fully open [29]. Moreover, the new FA VLCs identified in this study are polyunsaturated species and it must be emphasized that a recent study suggests that the poly-unsaturation of OAHFA acids can lead to loss of resistance to evaporation [30]. We thus hypothesize that, as VLC SFA, VLC PUFA may be involved in tear film stability. However, further studies are needed to fully understand the role of FA (32:3), FA (34:3) and FA (36:3) in meibum, especially in the context of dry eye disease. It is noteworthy that known VLC PUFA, including FA (32:6 ω -3) and FA (34:5 ω -3), have been previously detected in the retina within phospholipids where they play a key role in the visual function [9,31–33]. The question arises if retina also contains FA (32:3), FA (34:3) and FA (36:3).

4. Conclusion

The present study reports the identification in meibomian secretion of FA (32:3), FA (34:3) and FA (36:3). These three new VLC PUFA belong to the ω -3 family and, depending on the FA considered, have been detected as OAHFA, cholesteryl esters and, to a less extent, as free fatty acids. Chromatographic, MS and MS/MS data analysis were used to propose a reliable identification of these FA species. Double bond location was achieved using cross metathesis and tandem mass spectrometry. The presence of such VLC PUFA in meibum is undoubtedly related to ELOVL4 enzyme activity mediating FA elongation. The biological functions of these VLC PUFA, especially their role in ocular surface maintain and involvement in dry eye disease, remain to be investigated.

5. Author contribution

RM: Conceptualization, Methodology, Collection of data, Analysis of Data, Writing – Original Draft, AR: Conceptualization, Collection of data, Analysis of Data, Writing – Original Draft, KK: Collection of data, Analysis of Data, Writing – Review & Editing, OC: Collection of data, Analysis of Data, Writing – Original Draft, CB: Conceptualization, Supervision, Writing – Review & Editing, ER: Conceptualization, Methodology, Collection of data, Analysis of Data, Writing – Review & Editing, FB: Conceptualization, Supervision, Writing – Review & Editing, OL: Conceptualization, Supervision, Writing – Review & Editing, NA: Conceptualization, Methodology, Supervision, Writing – Original Draft.

Acknowledgements

This study was funded by Sorbonne Université, the Institut National de la Santé et de la Recherche Médicale and Centre National de la Recherche Scientifique. This work was completed with the support of the Programme Investissements d'Avenir IHU FOReSIGHT (ANR-18-IAHU-01). The authors thank the core facilities of the Institut de la vision, the Centre Hospitalier National d'Ophthalmologie des Quinze-Vingts, Région Ile-de-France and Ville de Paris.

Appendix A. Supplementary data

Supplementary data to this article can be found online at <https://doi.org/10.1016/j.biochi.2022.04.008>.

References

- [1] I.A. Butovich, T. Suzuki, J. Wojtowicz, N. Bhat, S. Yuksel, Comprehensive profiling of Asian and Caucasian meibomian gland secretions reveals similar lipidomic signatures regardless of ethnicity, *Sci. Rep.* 10 (2020) 14510, <https://doi.org/10.1038/s41598-020-71259-5>.
- [2] M.D.P. Willcox, P. Argüeso, G.A. Georgiev, J.M. Holopainen, G.W. Laurie, T.J. Millar, E.B. Papas, J.P. Rolland, T.A. Schmidt, U. Stahl, T. Suarez,

- L.N. Subbaraman, O. Uçakhan, L. Jones, TFOS DEWS II tear film report, *Ocul. Surf.* 15 (2017) 366–403, <https://doi.org/10.1016/j.jtos.2017.03.006>.
- [3] C. Baudouin, E.M. Messmer, P. Aragona, G. Geerling, Y.A. Akova, J. Benítez-Del-Castillo, K.G. Boboridis, J. Merayo-Llves, M. Rolando, M. Labetoulle, Revisiting the vicious circle of dry eye disease: a focus on the pathophysiology of meibomian gland dysfunction, *Br. J. Ophthalmol.* 100 (2016) 300–306, <https://doi.org/10.1136/bjophthalmol-2015-307415>.
- [4] S.M. Lam, L. Tong, S.S. Yong, B. Li, S.S. Chaurasia, G. Shui, M.R. Wenk, Meibum lipid composition in Asians with dry eye disease, *PLoS One* 6 (2011), <https://doi.org/10.1371/journal.pone.0024339>.
- [5] S.M. Lam, L. Tong, B. Reux, X. Duan, A. Petznick, S.S. Yong, C.B.S. Khee, M.J. Lear, M.R. Wenk, G. Shui, Lipidomic analysis of human tear fluid reveals structure-specific lipid alterations in dry eye syndrome, *J. Lipid Res.* 55 (2014) 299–306, <https://doi.org/10.1194/jlr.P041780>.
- [6] N. Yokoi, G.A. Georgiev, Tear film-oriented diagnosis and tear film-oriented therapy for dry eye based on tear film dynamics, *Invest. Ophthalmol. Vis. Sci.* 59 (2018), <https://doi.org/10.1167/jovs.17-23700>, DES13–DES22.
- [7] I.A. Butovich, Tear film lipids, *Exp. Eye Res.* 117 (2013) 4–27, <https://doi.org/10.1016/j.exer.2013.05.010>.
- [8] S.M. Lam, L. Tong, X. Duan, A. Petznick, M.R. Wenk, G. Shui, Extensive characterization of human tear fluid collected using different techniques unravels the presence of novel lipid amphiphiles, *J. Lipid Res.* 55 (2014) 289–298, <https://doi.org/10.1194/jlr.M044826>.
- [9] G.K. Yeboah, E.S. Lobanova, R.S. Brush, M.P. Agbaga, Very long chain fatty acid-containing lipids: a decade of novel insights from the study of ELOVL4, *J. Lipid Res.* 62 (2021) 100030, <https://doi.org/10.1016/j.jlr.2021.100030>.
- [10] H. Tanno, T. Sassa, M. Sawai, A. Kihara, Production of branched-chain very-long-chain fatty acids by fatty acid elongases and their tissue distribution in mammals, *Biochim. Biophys. Acta Mol. Cell Biol. Lipids* 1866 (2021) 158842, <https://doi.org/10.1016/j.bbalip.2020.158842>.
- [11] I.A. Butovich, Cholesteryl esters as a depot for very long chain fatty acids in human meibum, *J. Lipid Res.* 50 (2009) 501–513, <https://doi.org/10.1194/JLR.M800426-JLR200>.
- [12] R. Magny, A. Regazzetti, K. Kessal, G. Genta-Jouve, C. Baudouin, S. Mélik-Parsadaniantz, F. Brignole-Baudouin, O. Laprévote, N. Auzeil, Lipid annotation by combination of UHPLC-HRMS (MS), molecular networking, and retention time prediction: application to a lipidomic study of in vitro models of dry eye disease, *Metab.* 10 (2020) 225, <https://doi.org/10.3390/METAB10060225>, 2020, Vol. 10, Page 225.
- [13] R. Magny, N. Auzeil, E. Olivier, K. Kessal, A. Regazzetti, M. Dutot, S. Mélik-Parsadaniantz, P. Rat, C. Baudouin, O. Laprévote, F. Brignole-Baudouin, Lipidomic analysis of human corneal epithelial cells exposed to ocular irritants highlights the role of phospholipid and sphingolipid metabolisms in detergent toxicity mechanisms, *Biochimie* 178 (2020) 148–157, <https://doi.org/10.1016/j.biochi.2020.07.015>.
- [14] R. Magny, A. Regazzetti, K. Kessal, C. Baudouin, S. Mélik-Parsadaniantz, O. Laprévote, F. Brignole-Baudouin, N. Auzeil, E. Roulland, Deepening of lipidome annotation by associating cross-metathesis reaction with mass spectrometry: application to an in vitro model of corneal toxicity, *Anal. Bioanal. Chem.* 413 (2021) 4825–4836, <https://doi.org/10.1007/s00216-021-03438-w>.
- [15] O.D. Myers, S.J. Sumner, S. Li, S. Barnes, X. Du, One step forward for reducing false positive and false negative compound identifications from mass spectrometry metabolomics data: new algorithms for constructing extracted ion chromatograms and detecting chromatographic peaks, *Anal. Chem.* 89 (2017) 8696–8703, <https://doi.org/10.1021/acs.analchem.7b00947>.
- [16] J. Lanzini, D. Dargère, A. Regazzetti, A. Tebani, O. Laprévote, N. Auzeil, Changing in lipid profile induced by the mutation of Foxn1 gene: a lipidomic analysis of Nude mice skin, *Biochimie* 118 (2015) 234–243, <https://doi.org/10.1016/j.biochi.2015.09.029>.
- [17] R. Magny, K. Kessal, A. Regazzetti, A. Ben Yedder, C. Baudouin, S. Mélik-Parsadaniantz, F. Brignole-Baudouin, O. Laprévote, N. Auzeil, Lipidomic analysis of epithelial corneal cells following hyperosmolarity and benzalkonium chloride exposure: new insights in dry eye disease, *Biochim. Biophys. Acta Mol. Cell Biol. Lipids* 1865 (2020), <https://doi.org/10.1016/j.bbalip.2020.158728>.
- [18] L.F. Nothias, D. Petras, R. Schmid, K. Dührkop, J. Rainer, A. Sarvepalli, I. Protsyuk, M. Ernst, H. Tsugawa, M. Fleischauer, F. Aicheler, A.A. Aksenov, O. Alka, P.M. Allard, A. Barsch, X. Cachet, A.M. Caraballo-Rodríguez, R.R. Da Silva, T. Dang, N. Garg, J.M. Gauglitz, A. Gurevich, G. Isaac, A.K. Jarmusch, Z. Kameník, K. Bin Kang, N. Kessler, I. Koester, A. Korf, A. Le Gouellec, M. Ludwig, C. Martin H, L.I. McCall, J. McSayles, S.W. Meyer, H. Mohimani, M. Morsy, O. Moyné, S. Neumann, H. Neuweger, N.H. Nguyen, M. Nothias-Esposito, J. Paolini, V.V. Phelan, T. Pluskal, R.A. Quinn, S. Rogers, B. Shrestha, A. Tripathi, J.J.J. van der Hooft, F. Vargas, K.C. Weldon, M. Witting, H. Yang, Z. Zhang, F. Zubeil, O. Kohlbacher, S. Böcker, T. Alexandrov, N. Bandeira, M. Wang, P.C. Dorrestein, Feature-based molecular networking in the GNPS analysis environment, *Nat. Methods* 17 (2020) 905–908, <https://doi.org/10.1038/s41592-020-0933-6>.
- [19] F. Olivon, N. Elie, G. Grelier, F. Roussi, M. Litaudon, D. Touboul, MetGem software for the generation of molecular networks based on the t-SNE algorithm, *Anal. Chem.* 90 (2018) 13900–13908, <https://doi.org/10.1021/acs.analchem.8b03099>.
- [20] P. Shannon, A. Markiel, O. Ozier, N.S. Baliga, J.T. Wang, D. Ramage, N. Amin, B. Schwikowski, T. Ideker, Cytoscape: a software Environment for integrated models of biomolecular interaction networks, *Genome Res.* 13 (2003)

- 2498–2504, <https://doi.org/10.1101/gr.1239303>.
- [21] M. Miyamoto, T. Sassa, M. Sawai, A. Kihara, Lipid polarity gradient formed by ω -hydroxy lipids in tear film prevents dry eye disease, *Elife* 9 (2020), <https://doi.org/10.7554/ELIFE.53582>.
- [22] Q.F. Zhu, N. An, Y.Q. Feng, In-depth annotation strategy of saturated hydroxy fatty acids based on their chromatographic retention behaviors and MS fragmentation patterns, *Anal. Chem.* 92 (2020) 14528–14535, https://doi.org/10.1021/ACS.ANALCHEM.0C02719/SUPPL_FILE/AC0C02719_SI_001.PDF.
- [23] C. Hellmuth, M. Weber, B. Koletzko, W. Peissner, Nonesterified Fatty Acid Determination for Functional Lipidomics: Comprehensive Ultrahigh Performance Liquid Chromatography–Tandem Mass Spectrometry Quantitation, Qualification, and Parameter Prediction, 2012, <https://doi.org/10.1021/ac202602u>.
- [24] F. Aicheler, J. Li, M. Hoene, R. Lehmann, G. Xu, O. Kohlbacher, Retention time prediction improves identification in nontargeted lipidomics approaches, *Anal. Chem.* 87 (2015) 7698–7704, <https://doi.org/10.1021/acs.analchem.5b01139>.
- [25] M. Ovčáčíková, M. Lísa, E. Cífková, M. Holčapek, Retention behavior of lipids in reversed-phase ultrahigh-performance liquid chromatography-electrospray ionization mass spectrometry, *J. Chromatogr. A* 1450 (2016) 76–85, <https://doi.org/10.1016/j.chroma.2016.04.082>.
- [26] C.W.N. Damen, G. Isaac, J. Langridge, T. Hankemeier, R.J. Vreeken, Enhanced lipid isomer separation in human plasma using reversed-phase UPLC with ion-mobility/high-resolution MS detection, *J. Lipid Res.* 55 (2014) 1772, <https://doi.org/10.1194/jlr.D047795>.
- [27] S.H. Hong, M.W. Day, R.H. Grubbs, Decomposition of a key intermediate in ruthenium-catalyzed olefin metathesis reactions, *J. Am. Chem. Soc.* 126 (2004) 7414–7415, <https://doi.org/10.1021/ja0488380>.
- [28] L. Zhang, C.W. Borysenko, T.R. Lee, Kinetics of the cis,cis to trans,trans isomerization of 1,1,2,2,5,5,6,6-octamethyl-1,2,5,6-tetrasilacycloocta-3,7-diene, *J. Org. Chem.* 66 (2001) 5284–5290, <https://doi.org/10.1021/jo0014820>.
- [29] A. McMahon, H. Lu, I.A. Butovich, A role for ELOVL4 in the mouse meibomian gland and sebocyte cell biology, *Invest. Ophthalmol. Vis. Sci.* 55 (2014) 2832, <https://doi.org/10.1167/IOVS.13-13335>.
- [30] T. Viitaja, J.E. Raitanen, J. Moilanen, R.O. Paananen, F.S. Ekholm, The properties and role of O-Acyl- ω -hydroxy fatty acids and type I-st and type II diesters in the tear film lipid layer revealed by a combined chemistry and biophysics approach, *J. Org. Chem.* 86 (2021) 4965–4976, <https://doi.org/10.1021/acs.joc.0c02882>.
- [31] O. Berdeaux, P. Juaneda, L. Martine, S. Cabaret, L. Bretillon, N. Acar, Identification and quantification of phosphatidylcholines containing very-long-chain polyunsaturated fatty acid in bovine and human retina using liquid chromatography/tandem mass spectrometry, *J. Chromatogr. A* 1217 (2010) 7738–7748, <https://doi.org/10.1016/j.chroma.2010.10.039>.
- [32] B.R. Hopiavuori, R.E. Anderson, M.P. Agbaga, ELOVL4: very long-chain fatty acids serve an eclectic role in mammalian health and function, *Prog. Retin. Eye Res.* 69 (2019) 137–158, <https://doi.org/10.1016/j.preteyeres.2018.10.004>.
- [33] R. Harkewicz, H. Du, Z. Tong, H. Alkuraya, M. Bedell, W. Sun, X. Wang, Y.H. Hsu, J. Esteve-Rudd, G. Hughes, Z. Su, M. Zhang, V.S. Lopes, R.S. Molday, D.S. Williams, E.A. Dennis, K. Zhang, Essential role of ELOVL4 protein in very long chain fatty acid synthesis and retinal function, *J. Biol. Chem.* 287 (2012) 11469–11480, <https://doi.org/10.1074/jbc.M111.256073>.